Li *et al. Cellular & Molecular Biology Letters* (2025) 30:135
https://doi.org/10.1186/s11658-025-00822-7

Cellular & Molecular Biology Letters

RESEARCH ARTICLE Open Access

CDK5 regulates PPARγ/NF-κB signaling to exacerbate obesity-related osteoarthritis via modulating macrophage polarization and chondrocyte apoptosis

Yusheng Li[1,2], Hengzhen Li[1,2], Xin Chen[3,4], Xingfu Li[5], Jingyue Su[5], Shengwu Yang[3,4], Wenfeng Xiao[1,2*] and Zhenhan Deng[3,4,5*]

*Correspondence:
Wenfeng Xiao
xiaowenfeng@csu.edu.cn
Zhenhan Deng
dengzhenhan@wmu.edu.cn
[1]Department of Orthopedics, Xiangya Hospital, Central South University, Changsha 410008, Hunan, China
[2]National Clinical Research Center for Geriatric Disorders, Xiangya Hospital, Central South University, Changsha 410008, Hunan, China
[3]Department of Orthopedics, The First Affiliated Hospital of Wenzhou Medical University, Wenzhou 325000, Zhejiang, China
[4]Geriatrics Center, The First Affiliated Hospital of Wenzhou Medical University, Wenzhou 325000, Zhejiang, China
[5]Department of Sports Medicine, The First Affiliated Hospital of Shenzhen University, Shenzhen, Second People's Hospital, Shenzhen 518035, Guangdong, China

Abstract

Background Obesity is an important risk factor for osteoarthritis (OA), but the mechanisms associated with OA progression are still not fully understood. The aim of this study was to investigate the role of cyclin-dependent kinase 5 (CDK5) in regulating the peroxisome proliferator-activated receptor gamma (PPARγ)/nuclear factor-κB (NF-κB) signaling pathway and its effect on obesity-related OA.

Methods By analyzing tissue samples from obese and nonobese patients with OA in conjunction with a high-fat diet (HFD)-induced obese mouse model of OA, we investigated the expression level of CDK5 and its effects on inflammation and apoptosis. The role of CDK5 in macrophage polarization and chondrocyte apoptosis was further explored by gene knockdown and pharmacological intervention.

Results CDK5 levels were found to be significantly elevated in obese patients with OA, promoting M1 macrophage infiltration and chondrocyte apoptosis. In the model, CDK5 knockdown attenuated cartilage damage and inhibited PPARγ phosphorylation and NF-κB signaling. In vitro experiments showed that overexpression of CDK5 facilitated M1 macrophage polarization and chondrocyte apoptosis, and PPARγ agonists reversed these effects. Mechanically, CDK5 binds to PPARγ to regulate the NF-κB signaling pathway.

Conclusion CDK5 promotes the progression of obesity-associated OA through the PPARγ/NF-κB pathway and is a potential therapeutic target in OA, especially in obese patients.

Keywords CDK5, Obesity-related osteoarthritis, PPARγ/NF-κB signaling, Macrophage polarization, Chondrocyte apoptosis, High-fat diet

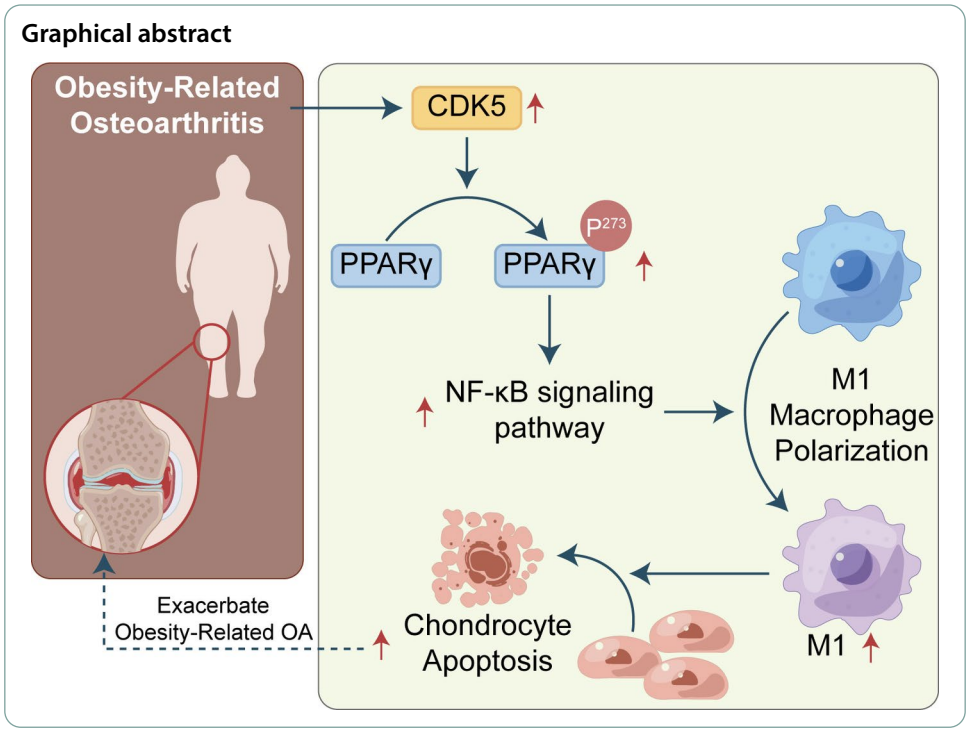

Introduction

Osteoarthritis (OA) and obesity are two major health issues in modern society. Obesity is associated with the incidence and progression of OA in joints such as the knee and hand. Obesity doubles the lifetime risk of symptomatic OA in comparison with individuals with a body mass index less than 25 [1]. The dynamic environment of the joints is repeatedly subjected to minor injury as a result of mobility, especially in joints that bear weight including the knees and hips, leading to ongoing wound healing and repair activities. This requires anabolic/catabolic enzyme activation within bones and cartilage [2, 3]. Typically, OA has been thought to be noninflammatory, caused by mechanical stress resulting in cartilage damage [4]. Nevertheless, OA is now widely characterized as a low-grade chronic inflammatory disease, evidenced by inflammatory cell infiltration in the synovium [5, 6].

Peroxisome proliferator-activated receptor gamma (PPAR-γ), a ligand-activated transcription factor crucial for lipid homeostasis, exerts a significant effect on modulating inflammation [7, 8]. As previously reported, PPAR-γ expression is dramatically decreased within both obese patients' infrapatellar fat pad and synovial membrane [9], which likely contributes to a proinflammatory and procatabolic environment within the joints, as the activation of PPAR-γ within adipose tissues is linked to favorable effects such as macrophage-induced suppression of proinflammatory cytokines such as resistin, interleukin (IL)–6, and tumor necrosis factor-α (TNF-α) [10]. Interestingly, cartilage-specific PPAR-γ knock-out mice develop spontaneous OA, indicating that PPAR-γ is vital for maintaining chondrocyte function and inhibiting pro-catabolic pathways by supporting autophagy [11, 12]. PPAR-γ agonists effectively reduce inflammation and catabolism within articular chondrocytes and synovial fibroblasts [13]. As recently reported, PPAR activation contributes to OA improvement by several agents/factors [14–17]. Therefore, the lower expression of PPAR-γ in obese patients' knee joint tissues

suggests the potential advantages of targeted treatment for this OA subgroup [18]. Previous studies have shown that inflammatory mediators in OA are regulated by nuclear factor-κB (NF-κB), a crucial transcription factor in inflammation. Reportedly, inhibition of NF-κB activation could attenuate OA development [19]. Activation of PPAR-γ could repress the inflammation, as demonstrated by the capacity of PPAR-γ agonists to inhibit the activation of NF-κB signaling and the release of proinflammatory cytokines induced by lipopolysaccharides [20, 21]. Given the significant decrease in PPAR-γ levels observed in obese individuals with OA, understanding the unknown mechanisms underlying this reduction could lead to targeted therapies that address the specific inflammatory pathways associated with obesity-related OA.

Cyclin-dependent kinase 5 (CDK5) is known to exert a significant effect on a variety of cellular processes, such as inflammation [22, 23]. Recent studies have identified CDK5 as a mediator of PPARγ phosphorylation at Ser273, which leads to a decrease in PPARγ activity [24, 25]. This reduction of PPARγ through CDK5-mediated phosphorylation at Ser273 impairs PPARγ's ability to regulate gene expression related to lipid metabolism and anti-inflammatory responses, thereby facilitating a pro-inflammatory state [24, 25]. Despite the established roles of CDK5 in inflammation and PPARγ regulation, the specific impact of CDK5-mediated PPARγ phosphorylation at Ser273 in the context of obesity-related OA remains largely unexplored. Notably, Zhang et al. [26] reported that CDK5 mRNA expression and protein levels were remarkably elevated within IL-1β-induced C28/I2 cells; CDK5 expression depletion inhibited the apoptosis, inflammatory response and extracellular matrix (ECM) in C28/I2 cells with IL-1β stimulation. Therefore, CDK5 has been thought to influence PPARγ activity and the subsequent inflammatory responses in obesity-related OA through PPARγ phosphorylation at Ser273, facilitating OA development.

In this study, OA lesions and CDK5 levels in obese patients were examined. The OA phenotypes and M1 macrophage infiltration in high-fat diet (HFD)-fed, destabilization of the medial meniscus (DMM)-induced OA mouse model were assessed. CDK5 was knocked down in the mouse model to investigate its effects on obesity-related OA cartilage damage and PPARγ/NF-κB signaling, as well as synovial M1 macrophage infiltration. The impact of CDK5 on free fatty acid-induced macrophage polarization in RAW264.7 cells and palmitic acid (PA)-induced chondrocyte damage was evaluated. Finally, the influence of PPAR-γ pathway inhibition on CDK5-mediated macrophage polarization and chondrocyte damage was examined. Collectively, the mechanisms by which CDK5 and PPARγ interactions contribute to inflammation and OA progression in obesity were elucidated to provide insights that could inform the development of targeted therapies for obesity-related OA.

Materials and methods

Patient samples

Synovial and cartilage tissues were harvested from six subjects without OA (aged 66.17 ± 5.00 years, one male and five female, body mass index [BMI] ≤ 24) undergoing traumatic amputation surgery, six nonobese OA subjects (Thin-OA, aged 64.33 ± 6.62 years, six female, BMI ≤ 24), and six obese OA subjects (Obesity-OA, aged 75.83 ± 9.24 years, four male and two female, BMI > 30) undergoing joint replacement surgery in Shenzhen Second People's Hospital. The clinical information is listed in

Supplementary Table S1. Specimens underwent immediate freezing within liquid nitrogen at −80 °C for subsequent analysis. This study was carried out under the approval of the institutional review board of Shenzhen Second People's Hospital, and all participants provided written informed consent.

Animal models

Male C57BL/6J mice (8 weeks old) were procured from Hunan SJA Laboratory Animal Co. Ltd and used for in vivo experiments. Mice were divided into six groups ($n = 9$ per group): Sham, HFD + Sham, DMM, HFD + DMM, HFD + DMM + Lv-sh-NC, and HFD + DMM + Lv-sh-CDK5. The DMM surgical procedure to establish the OA model is described in previous studies [27]. Both knees of mice underwent DMM surgery to induce OA. A xylazine/ketamine solution was injected intraperitoneally to anesthetize the animals. After anesthesia, the medial skin of the hindlimbs was disinfected using iodophor and alcohol. An aseptic medial capsular incision was made to expose the knee joint, then the medial meniscotibial ligament was resected to dislocate it. Before the DMM surgery, mice followed either a routine diet (15% energy from fat) or HFD (60% energy from fat) for 8 weeks. The Sham group was fed a standard diet and sham surgery, whereas the HFD + Sham group received a HFD for 8 weeks followed by sham surgery. DMM group received DMM surgery to induce OA. The HFD + DMM group received a HFD for 8 weeks followed by DMM surgery. For gene knockdown studies, the HFD + DMM + Lv-sh-NC and HFD + DMM + Lv-sh-CDK5 groups received intra-articular injections of 10 μL lentivirus packaged with short hairpin RNA (shRNA) of CDK5 (sh-CDK5) or negative control (sh-NC), respectively, at a dose of 1×10^8 PFU/mL every 2 weeks post-DMM surgery. Eight weeks after DMM surgery, mice were weighed and euthanized.The serum, epididymal fat, cartilage, and synovium were collected for further analysis. For histological analysis, six left knee joint sections were analyzed per group, and for western blot validation, right knee cartilage tissue from at least three mice per group was analyzed.

Primary chondrocytes isolation and culture

Primary chondrocytes were isolated from healthy wild-type C57BL/6J mice as previously described [28]. Briefly, articular cartilage was excised from knee joints, minced into < 1 mm^2 fragments, and digested in 0.1% collagenase I (17018029, Gibco, Grand Island, USA) at 37 °C for 4 h. The resulting cell suspension was seeded in T25 flasks containing Dulbecco's modified Eagle's medium/nutrient mixture F-12 (DMEM/F12; 11320033, Gibco) supplemented with 20% fetal bovine serum (FBS, Gibco), 100 U/mL penicillin, 100 μg/mL streptomycin, and 100 μg/mL gentamicin (Solarbio, Beijing, China). Cultures were maintained at 37 °C in a humidified 5% CO_2 incubator. Once chondrocytes migrated out from explants and reached > 80% confluency, medium was switched to DMEM/F12 with 10% FBS for experimental assays.

Cell culture and treatments

RAW264.7 macrophages (TIB-71) were obtained from the American Type Culture Collection (ATCC) (Manassas, USA) and cultivated in DMEM (30–2002, ATCC) containing 10% FBS and 1% penicillin/streptomycin (PS). After transfection with scrambled control of small interfering RNA (siRNA) (si-NC), siRNA of CDK5 (si-CDK5), overexpressed

control vector (Vector), or CDK5 overexpression (OE) plasmid (CDK5 OE), macrophages or chondrocytes were subjected to treatment with 0.5 mmol/L PA for 24 h in various experimental groups: Control, PA, PA + si-NC, PA + si-CDK5, PA + Vector, PA + CDK5 OE, and PA + CDK5 OE + Rosi (1 μM rosiglitazone).

Cell transfection

Transfections were performed using OriTrans® PEI-DNA (ORI2305, OriBio, Changsha, China) as per the instructions of the manufacturer. RAW264.7 cells or chondrocytes were subjected to transfection with si-NC, si-CDK5, empty vector, or CDK5 overexpression plasmids. For each well of a six-well plate, 4 μg of plasmid DNA or 40 pmol of siRNA was used. Cells were subjected to 6-h incubation with the transfection mixture, then the medium was replaced with fresh growth medium. Transfection efficiencies were confirmed using quantitative real-time reverse-transcriptase polymerase chain reaction (qRT-PCR). The sequences of overexpressing vector and siRNA sequence are listed in Supplementary Table S2.

Immunoblotting

Protein extracts from tissues and cultured cells were prepared with radioimmunoprecipitation assay (RIPA) lysis buffer containing protease and phosphatase inhibitors. Protein concentrations were determined using the bicinchoninic acid (BCA) protein assay kit (Thermo Fisher Scientific, Waltham, USA). Following electrophoresis by sodium dodecyl-sulfate polyacrylamide gel electrophoresis (SDS-PAGE), the separated proteins (30 μg) were electroblotted from the gel to polyvinylidene fluoride (PVDF) membranes. Membranes were subjected to 1-h blocking at room temperature (RT) using 5% skim milk in Tris-buffered saline with Tween 20 (TBS-T), followed by an overnight incubation at 4 °C using primary antibodies against CDK5 (10430-1-AP, Proteintech, Wuhan, China), reduced glyceraldehyde 3-phosphate dehydrogenase (GAPDH) (60004-1-IG, Proteintech), PPARγ (16643-1-AP, Proteintech), p-PPARγ (BS-4888R, Bioss, Woburn, USA), p65 (BF8005, Affinity, Changzhou, China), p-p65 (AF2006, Affinity), Aggrecan (DF7561, Affinity), collagen II (AF0135, Affinity), cleaved caspase-3 (25128-1-AP, Proteintech), Bax (50599-2-Ig, Proteintech), and Bcl2 (26593-1-AP, Proteintech). Membranes were washed, followed by 1-h incubation at RT using horseradish peroxidase (HRP)-labeled secondary antibodies. An enhanced chemiluminescence (ECL) detection system (Bio-Rad, Hercules, USA) was utilized to visualize protein bands. The intensity of protein bands was quantified with ImageJ software (National Institutes of Health, Bethesda, USA) and normalized to GAPDH.

Histological examination

Knee joint tissue samples were subjected to 48 h of fixing with 4% paraformaldehyde, 3 weeks of decalcification with 10% ethylenediaminetetraacetic acid (EDTA), paraffin embedding, and cutting into 5-μm slices. Slices were subjected to staining with hematoxylin and eosin (H&E) (C0105S, Beyotime, Shanghai, China) and Safranin O/Fast Green (G1053, Servicebio, Wuhan, China) as per the instructions of the manufacturer to evaluate histopathological changes. The Osteoarthritis Research Society International (OARSI) scoring system was employed to evaluate the severity of OA in the medial femoral condyle and medial tibial plateau [29]. Synovitis severity was estimated on the basis

of synovial lining cell layer enlargement, resident cell density, and inflammatory infiltration. A nine-point scale was used, where low scores indicated moderate synovitis and high scores represented severe synovitis [30]. The OARSI score and synovitis score were evaluated in blinded fashion by two independent pathologists.

Immunohistochemical (IHC) staining

After being deparaffinized and rehydrated, slices were subjected to antigen retrieval in citrate buffer (pH 6.0). Hydrogen peroxide (3%) was used to quench endogenous peroxidase activity. Next, slices were subjected to blocking with 5% bovine serum albumin (BSA), followed by overnight incubation at 4 °C using primary antibodies against cleaved caspase-3 (25128-1-AP, Proteintech) and inducible nitric oxide synthase (INOS) (22226-1-AP, Proteintech). Slices were washed, followed by incubation with biotinylated secondary antibodies. The avidin–biotin complex (ABC) kit (Vector Laboratories, Newark, USA) and 3,3′-diaminobenzidine (DAB) substrate were employed to visualize slices. The staining signals of targeted proteins were observed under light microscopy. The levels of cleaved caspase-3 and INOS were analyzed and quantified using ImageJ software.

Immunofluorescence (IF) staining

After being deparaffinized and rehydrated, slices were subjected to antigen retrieval. Slices were subjected to blocking with 5% BSA, followed by overnight incubation at 4 °C with primary antibodies against INOS (22226-1-AP, Proteintech). Slices were washed, followed by 1-h incubation in the dark at RT with Alexa Fluor 488-labeled secondary antibodies (Invitrogen). After counterstaining nuclei with 4′,6-diamidino-2-phenylindole (DAPI; Invitrogen), an antifade mounting medium was utilized to mount slices. A fluorescence microscope was applied to capture fluorescence images. The fluorescence intensity of INOS was analyzed and quantified using ImageJ software.

Flow cytometry

To assess macrophage polarization, RAW264.7 cells were harvested and stained with anti-INOS (12–5920-82, Invitrogen, Carlsbad, USA) and anti-CD206 (141706, Biolegend, San Diego, USA) antibodies. Cells were subjected to 30-min incubation at 4 °C away from light with antibodies, rinsed, and analyzed with a BD FACSCalibur flow cytometer.

Chondrocyte apoptosis was detected using Annexin-V/PI staining. Cells were subjected to staining with Annexin-V-fluorescein isothiocyanate (FITC) and propidium iodide (PI) as per the protocols of the manufacturer's instructions (BD Biosciences, San Jose, USA), and flow cytometry was employed to analyze. FlowJo software was applied to analyze data.

qRT-PCR

TRIzol reagent (Invitrogen) was employed to extract total RNA from tissue samples and cell lines. A Nanodrop spectrophotometer (Thermo Fisher Scientific) was employed to determine RNA concentrations. A High-Capacity cDNA Reverse Transcription Kit (Applied Biosystems, Waltham, USA) was utilized to synthesize cDNA from 1 μg of RNA. SYBR Green Master Mix (Applied Biosystems) on a QuantStudio 3 real-time PCR system (Applied Biosystems) was applied to perform qPCR. The following primers were used: CDK5, PPARγ, INOS, TNF-α, Arg-1, IL-10, and GAPDH (Supplementary Table

S2). The $2^{-\Delta\Delta Ct}$ method was employed to calculate relative gene expression levels, with normalization to GAPDH.

Serum biochemistry

Commercial kits (A110-1–1 for triglycerides (TG) and A111-1-1 for total cholesterol (T-CHO), Nanjing Jiancheng Bioengineering Institute, Nanjing, China) were used as per the protocols of the manufacturer to measure serum levels of TG and T-CHO. Cardiac puncture was utilized to collect blood specimens, and 15-min centrifugation (3000 rpm) at 4 °C was conducted to separate serum.

Co-immunoprecipitation (Co-IP) assay

RAW264.7 macrophages and chondrocytes were lysed in non-denaturing buffer. Protein concentration was measured using a BCA assay, and equal amounts (~ 500 μg) were incubated overnight at 4 °C with 2 μg of anti-CDK5 antibody or control immunoglobulin G (IgG). The complexes were captured using Protein A/G magnetic beads (P2108, Beyotime) for 2 h at 4 °C. After washing beads three times with lysis buffer, bound proteins were eluted in SDS sample buffer, resolved by SDS-PAGE, and analyzed via Western blot using anti-PPARγ and anti-CDK5 antibody. To assess the effect of Rosi, cells were pretreated with 1 μM Rosi for 24 h before lysis. All co-IP experiments were conducted in biological triplicates. Input and IgG controls were included to confirm specificity.

Chromatin immunoprecipitation (ChIP)

Crosslinked chromatin from RAW264.7 macrophages or chondrocytes (~5×10^6 cells) was sonicated to ~200–500 bp fragments. Immunoprecipitation was performed using anti-PPARγ antibody or control IgG incubation overnight, with complexes captured on Protein A/G magnetic beads (P2080S, Beyotime). Following sequential low/high-salt washes, DNA–protein crosslinks were reversed, and DNA was purified using a standard Clean Up kit (D0041S, Beyotime). Enrichment of PPARγ binding at predicted sites within the IκBα promoter (~2.0 kb upstream) was assessed via qPCR and calculated as percentage input using the ΔCt method. Each condition was performed in biological triplicates.

Luciferase reporter assay

To assess the effect of CDK5 on IκBα promoter transcriptional activity, a 2.0-kb fragment of the mouse IκBα promoter (– 2000 to + 1 bp relative to the transcription start site) was cloned upstream of the firefly luciferase gene in the psicheck-2 vector (psicheck-2-IκBα-Luc). RAW264.7 macrophages or chondrocytes were seeded in 24-well plates and co-transfected with psicheck-2-IκBα-Luc, 50 ng of *Renilla* luciferase control plasmid, and CDK5 OE or empty vector. After 24 h, cells were treated with or without 1 μM Rosi for an additional 24 h. Firefly and *Renilla* luciferase activities were measured using the Dual-Luciferase Reporter System (Promega, Madison, USA). The primers for vector construction are listed in Supplementary Table S2.

Statistical analysis

The cell experiments were performed at least three times. The animal experiments were performed at least six times. GraphPad Prism 8.0 software (GraphPad Software, San

Diego, USA) was applied to analyze all data. Results are presented as mean ± standard deviation (SD) of at least three independent experiments. The Shapiro–Wilk test was utilized to assess the data distribution normality. For normally distributed data, one-way analysis of variance (ANOVA) followed by Tukey's post hoc test was performed to assess differences among groups, and Student's *t*-test was conducted to assess differences between groups. The Kruskal–Wallis test followed by Dunn's post hoc test was applied to analyze non-normally distributed data. A *p*-value greater than 0.05 means that no significant effect was observed.

Results

Increased severity of OA lesions and elevated CDK5 levels in obese patients with OA

Synovial and cartilage samples were collected from participants without OA (control), nonobese patients with OA (Thin-OA), and obese patients with OA (Obesity-OA). H&E staining revealed distinct cartilage morphologies across the groups: samples from patients in the Thin-OA group exhibited superficial erosion of the articular surface, while Obesity-OA samples showed more extensive degradation, including deeper cartilage loss and a marked reduction in chondrocyte granules. In contrast, cartilage from healthy controls maintained a smooth articular surface with abundant chondrocyte granules (Fig. 1A). The OARSI scores were consistent with histological findings, which revealed that Thin-OA group had significantly higher cartilage scores compared with healthy control group, while the Obesity-OA group had highest OARSI score (Fig. 1B). The severity of synovial inflammation and hyperplasia was progressively increased across the groups. Control samples exhibited normal synovial architecture with minimal inflammation. In contrast, the Thin-OA group showed moderate synovial hyperplasia, inflammatory cell infiltration, and higher synovitis score, while the Obesity-OA group displayed pronounced synovial thickening, severe inflammatory infiltration, and highest synovitis score, indicating a significant exacerbation of synovial pathology in obese patients with OA (Fig. 1C, D). CDK5 levels were significantly elevated in both synovial and cartilage tissues of the patients in the Obesity-OA group in comparison with normal controls and patients in the Thin-OA group (Fig. 1C, D).

HFD-induced obesity exacerbates DMM-induced OA and M1 macrophage infiltration in mice

Mice were allocated at random into four groups: Sham, HFD + Sham, DMM, and HFD + DMM. The OA model was established in mice as described, with a normal diet or HFD administered to model mice. Metabolic parameters were first evaluated in mice. The body weight was significantly increased in the HFD + Sham mice relative to the Sham mice (Supplementary Fig. S1A). The HFD + DMM group also exhibited a remarkable increase relative to the DMM mice (Supplementary Fig. S1A). The impact of HFD on lipid metabolism was assessed by measuring serum TG and T-CHO levels. Compared with the Sham group, HFD + Sham showed significantly elevated TG and T-CHO; compared with the DMM group, HFD + DMM group saw remarkably increased TG and T-CHO levels as well (Supplementary Fig. S1B). Consistently, H&E staining of epididymal fat pads revealed that adipocytes were remarkably larger within the HFD + Sham mice relative to the Sham mice, and the HFD + DMM group also showed enlarged

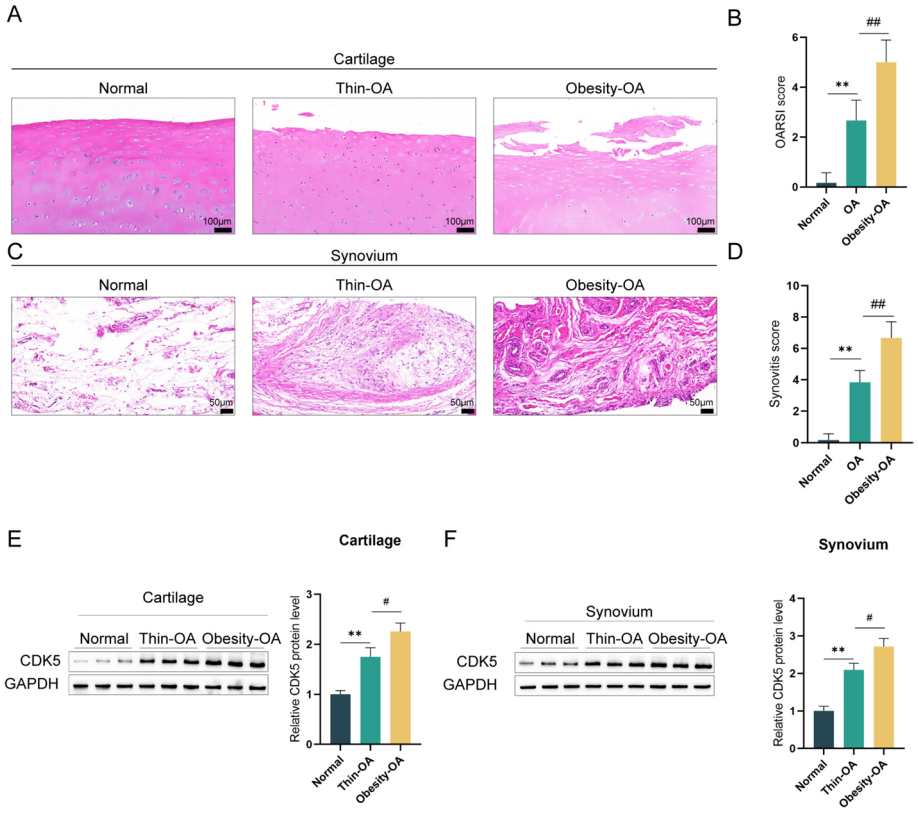

Fig. 1 Increased severity of OA lesions and elevated CDK5 levels in obese patients with OA. Synovial and cartilage samples were collected from six participants without OA (control), six nonobese patients with OA (Thin-OA), and six obese patients with OA (Obesity-OA). **A** H&E staining was performed on cartilage tissues to evaluate the severity of cartilage degradation and OA pathology. **B** The severity of articular cartilage damage was evaluated using the Osteoarthritis Research Society International (OARSI) scoring system. **C** H&E staining was performed on synovial tissue samples to evaluate the severity of synovial inflammation and hyperplasia. **D** The quantification of synovitis score was evaluated the synovitis severity of synovial tissues. $N = 6$. **E**, **F** Immunoblotting was performed to examine CDK5 levels in synovial and cartilage tissues. $N = 3$ (biological replicates). $^{**}p < 0.01$; $\#p < 0.05$

adipocytes compared with the DMM group, supporting the serum lipid level findings and indicating adipose tissue hypertrophy as a response to HFD (Supplementary Fig. S1C).

The severity of cartilage degradation and OA pathology was evaluated by performing H&E staining upon cartilage tissues. The results showed that the Sham group exhibited normal cartilage structure with no signs of degradation. In contrast, the HFD + Sham group displayed slight cartilage alterations, while the DMM group showed moderate cartilage degradation and OA pathology. The HFD + DMM group exhibited the most severe cartilage degradation and OA pathology, indicating that HFD-induced obesity exacerbates the severity of DMM-induced OA (Fig. 2A). There were no significant differences in knee OA OARSI scores between Sham and HFD + Sham group. However, the OARSI score was significantly elevated in DMM and HFD + DMM group, with the HFD + DMM group having the highest OARSI score (Fig. 2E). Proteoglycan loss and cartilage matrix degradation were assessed by performing Safranin O/Fast Green staining of cartilage tissues. Control samples from the Sham group displayed intact cartilage matrix with significant Safranin O staining, indicating elevated proteoglycan levels. The HFD + Sham group showed mild proteoglycan loss, while the DMM group exhibited moderate degradation of the cartilage matrix. The HFD + DMM group displayed extensive loss of

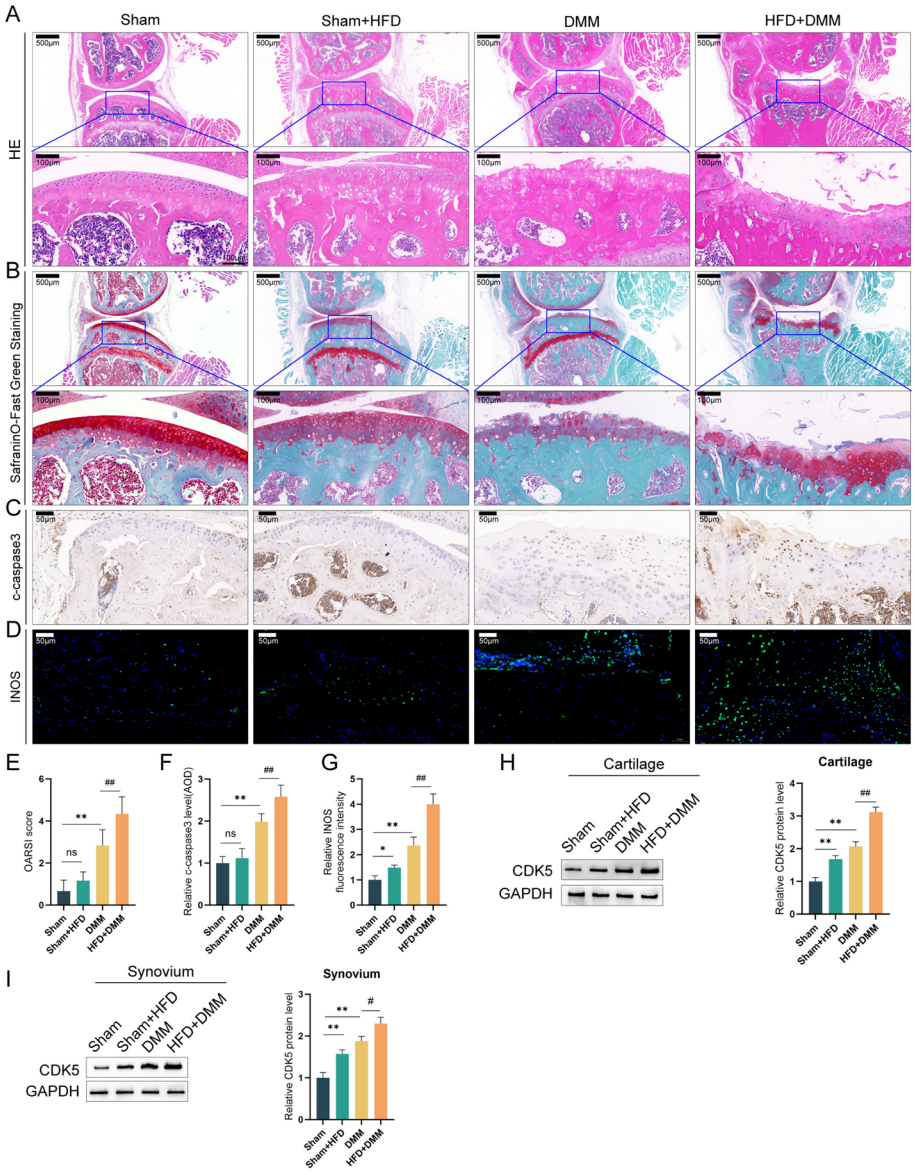

Fig. 2 HFD-induced obesity exacerbates DMM-induced OA and M1 macrophage infiltration in mice. Mice were randomly allocated into four groups: Sham, HFD + Sham, DMM, and HFD + DMM groups, and the OA model was established in mice as described; normal diet or HFD was administered to model mice. **A** H&E staining was performed on cartilage tissue samples to evaluate the severity of cartilage degradation and OA pathology. **B** Safranin O/Fast Green staining was performed on cartilage tissues to assess proteoglycan loss and cartilage matrix degradation. **C** IHC staining for cleaved caspase-3 was conducted on cartilage tissue samples to evaluate apoptosis. **D** IF staining was performed to detect INOS + cells in synovial tissues to assess M1 macrophage infiltration. **E** The severity of articular cartilage damage was evaluated using the OARSI scoring system. **F** Quantification of cleaved caspase-3 positive cell intensity based on the IHC staining of the cartilage tissues. **G** Quantification of INOS fluorescence intensity based on the IF staining of the cartilage tissues. **H**, **I** Immunoblotting was performed to determine CDK5 levels in cartilage and synovial tissues. $N = 6$ (biological replicates) for **A**–**G** and $N = 3$ (biological replicates) for **H** and **I**. $^{**}p < 0.01$; $\#p < 0.05$, $\#\#p < 0.01$

Safranin O staining and remarkable structural damage to the cartilage matrix, further confirming that obesity worsens DMM-induced cartilage degradation (Fig. 2B).

IHC staining for cleaved caspase-3 was conducted on cartilage tissue samples to evaluate apoptosis. The Sham and HFD + Sham group showed minimal cleaved caspase-3 staining, indicating low levels of apoptosis. The DMM group showed a more pronounced

increase with cleaved caspase-3-positive cells. The HFD + DMM group exhibited a remarkable increase of cleaved caspase-3 staining relative to the other groups, suggesting that HFD-induced obesity exacerbates apoptosis in DMM-induced OA (Fig. 2C, F).

IF staining was performed to detect $INOS^+$ cells in synovial tissues and assess M1 macrophage infiltration. The Sham group showed low levels of $INOS^+$ cells. The HFD + Sham group had a moderate increase in $INOS^+$ cells, while the DMM group displayed a remarkable increase within M1 macrophage infiltration. The HFD + DMM group exhibited the highest levels of $INOS^+$ cells, indicating that obesity significantly enhances M1 macrophage infiltration in the context of DMM-induced OA (Fig. 2D, G).

Immunoblotting was performed to determine CDK5 levels within cartilage and synovial tissue samples. The results showed low CDK5 expression levels within the cartilage and synovial tissue samples in the Sham mice. The HFD + Sham mice exhibited a slight elevation within CDK5 levels, while the DMM group showed a moderate increase. The HFD + DMM group displayed the highest CDK5 expression levels within both cartilage and synovial tissue samples, suggesting that HFD-induced obesity significantly upregulates CDK5 in cartilage and synovial tissues in DMM-induced OA (Fig. 2H, 2I). These data suggest that obesity exacerbates DMM-induced OA in mice and increases CDK5 levels.

CDK5 knockdown inhibits obesity-related osteoarthritis cartilage damage and modulates the PPARγ/NF-κB pathway

To investigate the effect of CDK5 knockdown upon obesity-associated OA cartilage damage and the modulation of PPARγ/NF-κB signaling, model mice were injected with negative control lentivirus (Lv-sh-NC) or lentivirus containing short hairpin RNA targeting CDK5 (Lv-sh-CDK5). The protein level of CDK5 in cartilage and synovial tissues was detected by Immunoblotting. CDK5 knockdown significantly reduced the levels of CDK5 in cartilage and synovial tissues, indicating good transfection efficiency (Supplementary Fig. S2A, B). H&E staining of cartilage tissue showed a significant reduction in cartilage damage in the HFD + DMM + Lv-sh-CDK5 group compared with the HFD + DMM and HFD + DMM + Lv-sh-NC groups (Fig. 3A). The OARSI score was significantly reduced in the HFD + DMM + Lv-sh-CDK5 group when compared with the HFD + DMM and HFD + DMM + Lv-sh-NC groups (Fig. 3B). Similarly, Safranin O/Fast Green staining revealed that the HFD + DMM + Lv-sh-CDK5 group exhibited less cartilage degradation compared with the HFD + DMM and HFD + DMM + Lv-sh-NC groups (Fig. 3C). IHC staining for cleaved caspase-3 in cartilage tissue indicated that the HFD + DMM + Lv-sh-CDK5 group exhibited a dramatically reduced level of apoptosis in comparison with the HFD + DMM and HFD + DMM + Lv-sh-NC groups (Fig. 3D, E). CDK5 knockdown markedly elevated aggrecan and collagen II proteins in mice cartilage tissues compared with the HFD + DMM and HFD + DMM + Lv-sh-NC groups (Fig. 3F). Immunoblotting also demonstrated that p-PPARγ (Ser273) and p-p65 levels were considerably reduced within the HFD + DMM + Lv-sh-CDK5 group compared with the HFD + DMM and HFD + DMM + Lv-sh-NC groups, suggesting that CDK5 knockdown suppressed the phosphorylation of PPARγ at Ser273, as well as p65 phosphorylation (Fig. 3G).

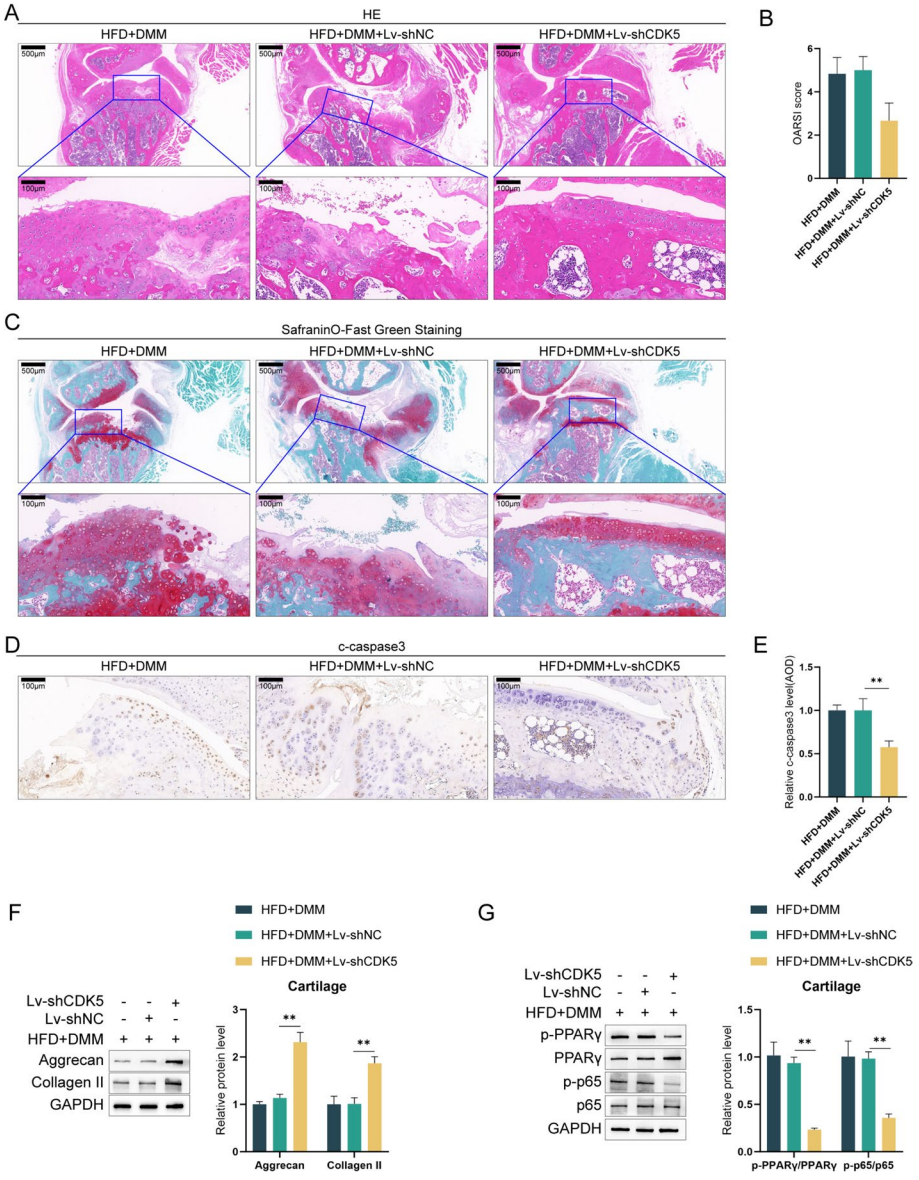

Fig. 3 CDK5 knockdown inhibits obesity-related osteoarthritis cartilage damage and modulates the PPARγ/NF-κB pathway. Mice were randomly allocated into three groups: HFD + DMM, HFD + DMM + lv-shNC, and HFD + DMM + lv-shCDK5 groups. **A** H&E staining of cartilage tissue from different groups of mice. **B** The severity of articular cartilage damage was evaluated using the OARSI scoring system. **C** Safranin O/Fast Green staining of cartilage tissue from different groups of mice. **D** IHC staining of cleaved caspase-3 in mouse cartilage tissue. **E** Quantification of cleaved caspase-3-positive cell intensity based on the IHC staining of the cartilage tissues. **F** Immunoblotting of aggrecan and collagen II protein levels in mouse cartilage tissue. **G** Immunoblotting of PPARγ, p-PPARγ (Ser273), p65, and p-p65 protein levels in cartilage tissue from different groups of mice. $N = 6$ (biological replicates) for **A**–**D** and $N = 3$ (biological replicates) for **F** and **G**. $^{**}p < 0.01$

CDK5 knockdown inhibits M1 macrophage infiltration and modulates the PPARγ/NF-κB pathway in synovial tissues of obesity-related OA mice

To explore the effect of CDK5 knockdown upon synovial M1 macrophage infiltration and the modulation of PPARγ/NF-κB signaling in synovial tissues of obesity-related OA mice, related factors were examined in synovial tissues. Significantly lower synovial INOS levels were revealed in the HFD + DMM + Lv-sh-CDK5 group by IF staining compared with the HFD + DMM and HFD + DMM + Lv-sh-NC groups (Fig. 4A, B).

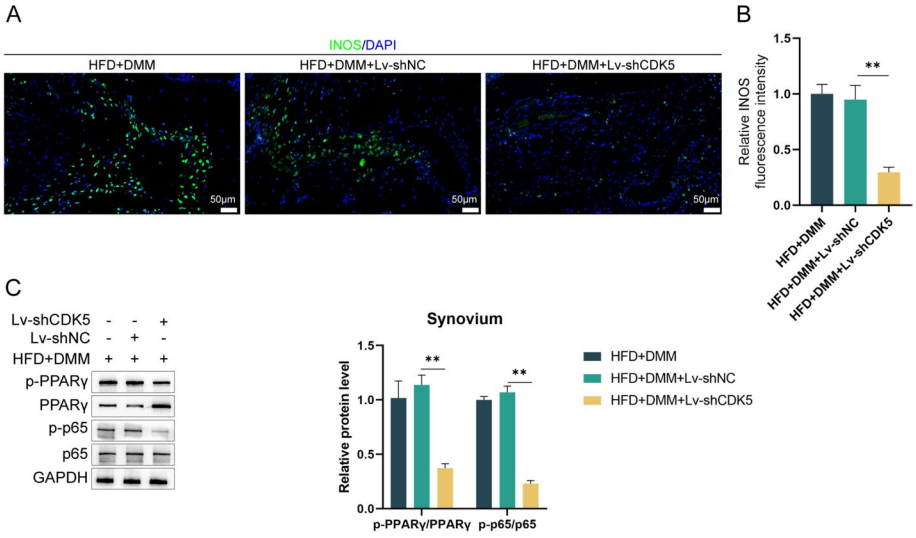

Fig. 4 CDK5 knockdown inhibits M1 macrophage infiltration and modulates the PPARγ/NF-κB pathway in synovial tissues of obesity-related OA mice. **A** IF staining of INOS levels in mouse synovial tissues. **B** Quantification of INOS fluorescence intensity based on IF staining of the synovial tissues. **C** Immunoblotting of PPARγ, p-PPARγ (Ser273), p65, and p-p65 protein levels in synovial tissue from different groups of mice. $N = 6$ (biological replicates) for **A** and **B** and $N = 3$ (biological replicates) for **C**. $^{**}p < 0.01$

Consistently, the levels of p-PPARγ (Ser273) and p-p65 were reduced in mice synovial tissues from the HFD + DMM + Lv-sh-CDK5 group compared with the HFD + DMM and HFD + DMM + Lv-sh-NC groups (Fig. 4C), suggesting that CDK5 knockdown could significantly inhibit synovial M1 macrophage infiltration and modulate the PPARγ/NF-κB pathway in the synovial tissues of mice.

CDK5 affects palmitic acid (PA)-induced macrophage polarization

To explore the effect of CDK5 upon PA-induced macrophage polarization and chondrocyte damage in vitro, small interfering RNA (siRNA) against CDK5 (siCDK5#1/2/3) or plasmid overexpressing CDK5 (CDK5 OE) was transfected into RAW264.7 macrophages and chondrocytes; CDK5 knockdown and overexpression were detected by qRT-PCR (Supplementary Fig. S2C–F). siCDK5#1 was used in the following experiments owing to its better interference efficiency (Supplementary Fig. S2E, F).

Next, RAW264.7 macrophages were transfected with siCDK5 or CDK5 OE and evaluated for macrophage polarization. qRT-PCR showed that PA treatment significantly increased the mRNA expression of both M1 (INOS and TNF-α) and M2 (Arg-1 and IL-10) polarization markers compared with the control group (Fig. 5A). CDK5 knockdown (PA + siCDK5) reduced the expression levels of M1 markers (INOS and TNF-α) compared with the PA and PA + si-NC groups, while CDK5 overexpression (PA + CDK5 OE) further increased M1 marker levels in comparison with the PA and PA + vector groups (Fig. 5A). Conversely, M2 marker levels were increased within the CDK5 knockdown group in comparison with the PA and PA + si-NC groups, but reduced within the CDK5 overexpression group in comparison with the PA and PA + vector groups (Fig. 5A). Flow cytometry (FC) analysis indicated that PA treatment dramatically increased the $INOS^+$ M1 macrophage percentage in comparison with normal controls; under PA treatment, CDK5 knockdown reduced the $INOS^+$ M1 macrophage percentage in comparison with the PA and PA + si-NC groups, while CDK5 overexpression increased the M1

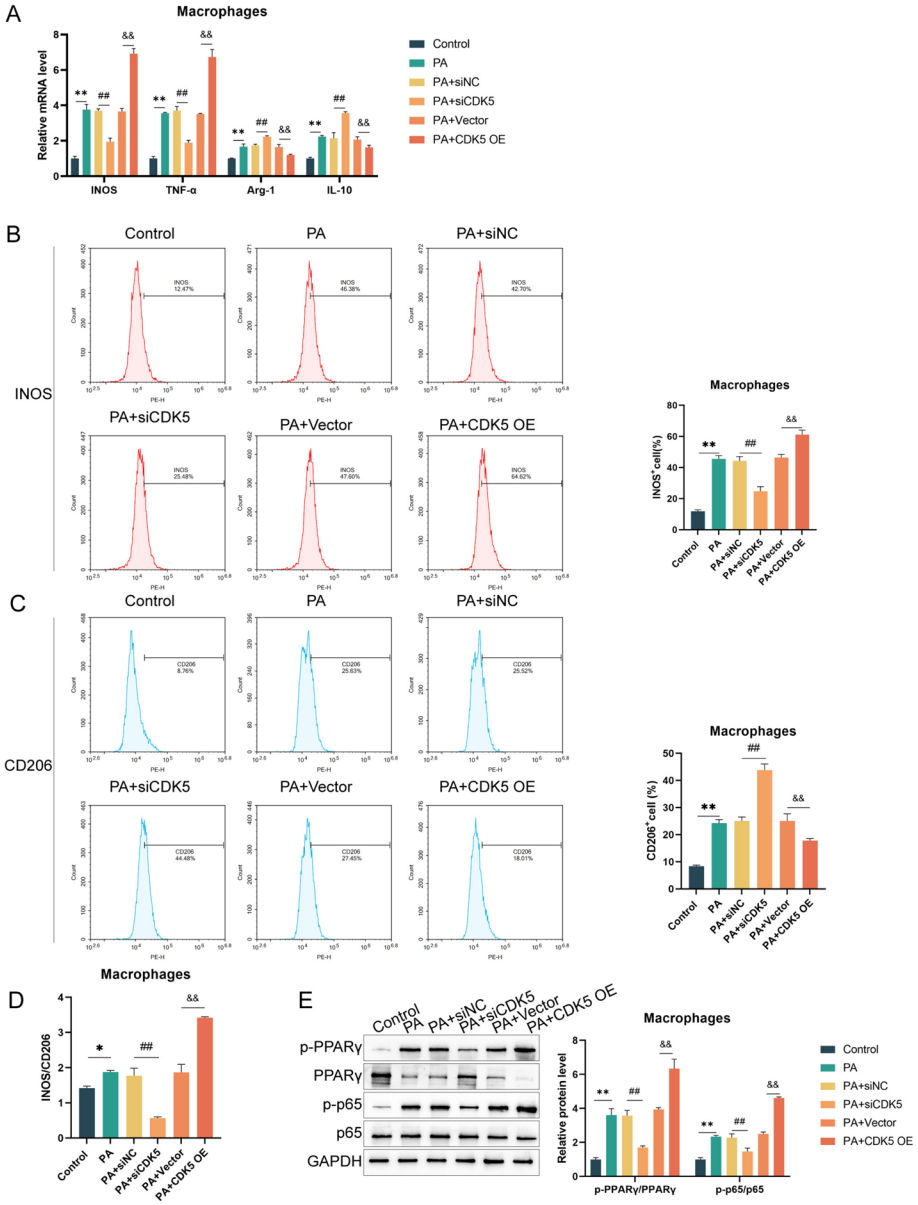

Fig. 5 CDK5 affects PA-induced macrophage polarization. Mouse macrophage RAW264.7 cells were transfected with siCDK5 or CDK5 OE. **A** qRT-PCR was performed to examine INOS and TNF-α (M1 polarization markers), Arg-1, and IL-10 (M2 polarization markers) mRNA levels in macrophages. **B** FC analysis of $INOS^+$ macrophages to evaluate macrophage M1 polarization. **C** FC analysis of $CD206^+$ macrophages to evaluate macrophage M2 polarization. **D** Calculation of INOS/CD206 levels to determine macrophage polarization. **E** Immunoblotting was performed to determine PPARγ, p-PPARγ (Ser273), p-p65, and p65 protein levels in macrophages. All $N = 3$ (biological replicates). $^*p < 0.05$, $^{**}p < 0.01$; $\#\#p < 0.01$; $\&\&p < 0.01$

macrophage percentage compared with the PA and PA + vector groups (Fig. 5B). Similarly, PA treatment also remarkably elevated the $CD206^+$ M2 macrophage percentage in comparison with normal controls; under PA treatment, CDK5 knockdown elevated the $CD206^+$ M2 macrophage percentage in comparison with the PA and PA + si-NC groups, while CDK5 overexpression decreased the $CD206^+$ M2 macrophage percentage compared with the PA and PA + vector groups (Fig. 5C). The ratio of INOS/CD206 was calculated to assess macrophage polarization. Compared with the control group, PA treatment elevated the INOS/CD206 ratio (Fig. 5D). CDK5 knockdown resulted in

a lower INOS/CD206 ratio in comparison with the PA and PA + si-NC groups, indicating a shift toward M2 polarization. In contrast, CDK5 overexpression led to a higher INOS/CD206 ratio, indicating a shift toward M1 polarization (Fig. 5D). Immunoblotting revealed that PA treatment facilitated the PPARγ at Ser273 phosphorylation and p65 phosphorylation compared with the control group (Fig. 5E). CDK5 knockdown suppressed, whereas CDK overexpression facilitated the PPARγ at Ser273 phosphorylation and p65 phosphorylation compared with the PA and PA + si-NC/Vector groups (Fig. 5E). Taken together, CDK5 exerts a significant effect on modulating macrophage polarization upon PA treatment, possibly through PPARγ/NF-κB signaling.

CDK5 affects PA-induced chondrocyte damage

To explore the effect of CDK5 upon PA-elicited chondrocyte damage, primary mouse chondrocytes were transfected with siCDK5 or CDK5 OE under PA treatment and examined for related indexes. FC analysis revealed that PA treatment significantly increased chondrocyte apoptosis compared with the Control group. Under PA treatment, CDK5 knockdown reduced apoptosis levels compared with the PA and PA + si-NC groups, while CDK5 overexpression further increased apoptosis levels (Fig. 6A). Consistently, PA treatment elevated the cleaved caspase-3 levels and the Bax/Bcl-2 ratio compared with the Control group. Under PA treatment, CDK5 knockdown decreased the cleaved caspase-3 levels and Bax/Bcl-2 ratio in comparison with the PA and PA + si-NC groups. Conversely, CDK5 overexpression further increased cleaved caspase-3 levels and Bax/Bcl-2 ratio (Fig. 6B). Immunoblotting for PPARγ, p-PPARγ (Ser273), p-p65, and p65 revealed that, under PA treatment, CDK5 knockdown suppressed PPARγ phosphorylation at Ser273 and p65 phosphorylation in chondrocytes compared with the PA and PA + si-NC groups, whereas CDK5 overexpression had the opposite effect, with enhanced PPARγ phosphorylation at Ser273 and p65 phosphorylation (Fig. 6C). In summary, CDK5 exerts a crucial effect on regulating chondrocyte apoptosis and damage in response to PA; the PPARγ/NF-κB pathway could also be involved.

PPARγ/NF-κB signaling mediates effects of CDK5 on PA-induced macrophage polarization

To investigate the effect of PPARγ/NF-κB signaling in mediating the effects of CDK5 on PA-induced macrophage polarization, PA-treated RAW264.7 cells were transfected with CDK5 OE with or without treatment with rosiglitazone (Rosi), a PPARγ agonist that inhibits PPARγ phosphorylation at Ser273. qRT-PCR analysis revealed that, in PA-treated macrophages, CDK5 OE further elevated the levels of M1 markers compared with the PA and PA + Vector groups, while Rosi treatment (PA + CDK5 OE + Rosi) reduced these markers induced by CDK5 OE. Conversely, CDK5 OE decreased the levels of M2 markers (Arg-1 and IL-10), while Rosi treatment further increased these levels (Fig. 7A). Consistently, FC analysis of $INOS^+$ macrophages indicated that CDK5 OE dramatically elevated the M1 macrophage percentage in comparison with the PA and PA + Vector mice. Rosi treatment decreased the M1 macrophage percentage within the CDK5 OE group (Fig. 7B). In addition, CDK5 OE decreased the percentage of M2 macrophages in comparison with the PA and PA + Vector mice. Rosi treatment elevated the M2 macrophage percentage in the CDK5 OE group (Fig. 7C). The INOS/CD206 ratio was calculated to assess macrophage polarization; CDK5 OE resulted in a higher INOS/CD206 ratio in comparison with the PA and PA + Vector mice, whereas Rosi treatment

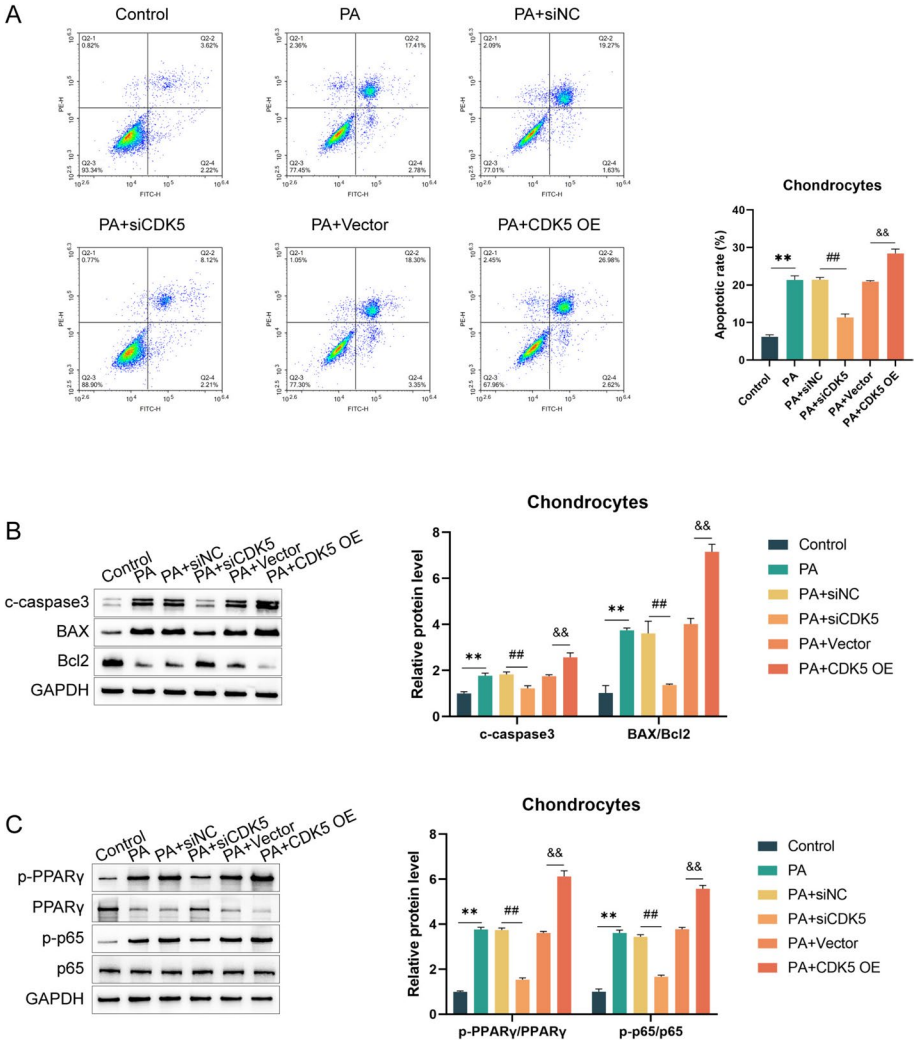

Fig. 6 CDK5 affects PA-induced chondrocyte damage. Mouse chondrocytes were transfected with siCDK5 or CDK5 OE. **A** FC was performed to determine cell apoptosis. **B** Immunoblotting was performed to determine the protein levels of cleaved-caspase3, Bax, and Bcl2. **C** Immunoblotting was performed to determine PPARγ, p-PPARγ (Ser273), p-p65, and p65 protein levels in chondrocytes. All $N = 3$ (biological replicates). $^{**}p < 0.01$; $\#\#p < 0.01$; $\&\&p < 0.01$

reduced the INOS/CD206 ratio in the CDK5 OE group, indicating a shift toward M2 polarization (Fig. 7D). Furthermore, CDK5 OE elevated p-PPARγ (Ser273) and p-p65 levels within macrophages compared with the PA and PA + Vector groups, whereas Rosi treatment reduced p-PPARγ (Ser273) and p-p65 levels within the CDK5 OE group, suggesting that Rosi suppressed CDK5 overexpression-induced PPARγ phosphorylation at Ser273 and p65 phosphorylation (Fig. 7E). In summary, PPARγ/NF-κB signaling mediates the effects of CDK5 upon PA-induced macrophage polarization, with CDK5 promoting M1 polarization and Rosi treatment mitigating these effects by inhibiting PPARγ phosphorylation.

PPARγ/NF-κB signaling mediates effects of CDK5 on PA-induced chondrocyte damage

To explore the effect of PPARγ/NF-κB signaling on mediating the effects of CDK5 upon PA-induced chondrocyte damage, PA-treated primary mouse chondrocytes were transfected with CDK5 OE with or without treatment with Rosi and examined for

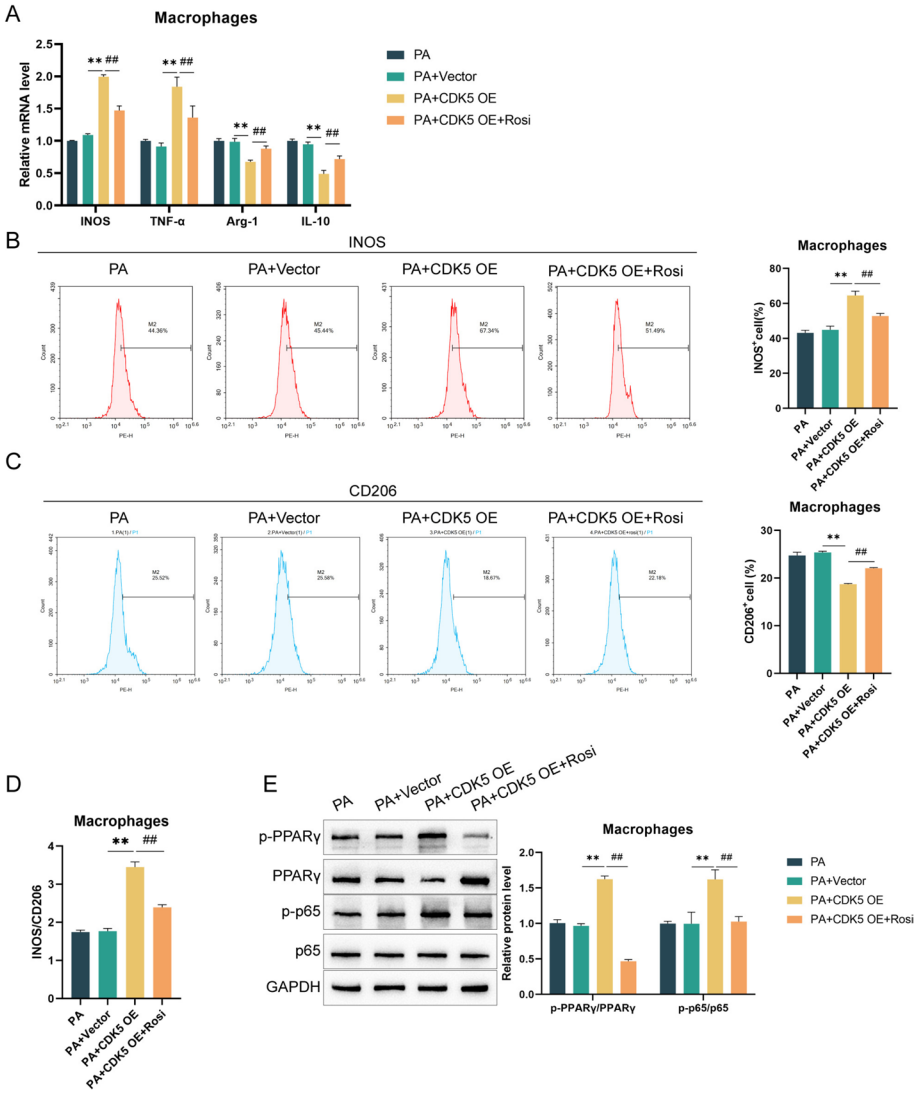

Fig. 7 PPARγ/NF-κB signaling mediates effects of CDK5 on PA-induced macrophage polarization. Under PA induction, mouse macrophage RAW264.7 cells were transfected with CDK5 OE with or without treatment with Rosi (a PPARγ agonist inhibiting PPARγ phosphorylation at Ser273). **A** qRT-PCR was performed to examine INOS and TNF-α (M1 polarization markers), Arg-1, and IL-10 (M2 polarization markers) mRNA levels in macrophages. **B** FC analysis of $INOS^+$ macrophages to evaluate macrophage M1 polarization. **C** FC analysis of $CD206^+$ macrophages to evaluate macrophage M2 polarization. **D** Calculation of INOS/CD206 levels to determine macrophage polarization. **E** Immunoblotting was performed to determine PPARγ, p-PPARγ (Ser273), p-p65, and p65 protein levels in macrophages. All $N = 3$ (biological replicates). $^{**}p < 0.01$; $^{\#\#}p < 0.01$

related indexes. Under PA treatment, CDK5 overexpression further increased apoptosis, while Rosi treatment (PA + CDK5 OE + Rosi) reduced the apoptosis compared with the PA + CDK5 OE group (Fig. 8A). Regarding apoptotic markers, CDK5 overexpression further increased cleaved caspase-3 levels and Bax/Bcl-2 ratio. Rosi treatment mitigated these effects, showing lower cleaved caspase-3 levels and Bax/Bcl-2 ratio compared with the PA + CDK5 OE chondrocytes (Fig. 8B). Immunoblotting for PPARγ, p-PPARγ (Ser273), p-p65, and p65 revealed that CDK5 overexpression elevated p-PPARγ (Ser273) and p-p65 levels within chondrocytes in comparison with the PA and PA + Vector group, whereas Rosi treatment decreased p-PPARγ (Ser273) and p-p65 levels compared with the PA + CDK5 OE group, suggesting that Rosi suppressed CDK5

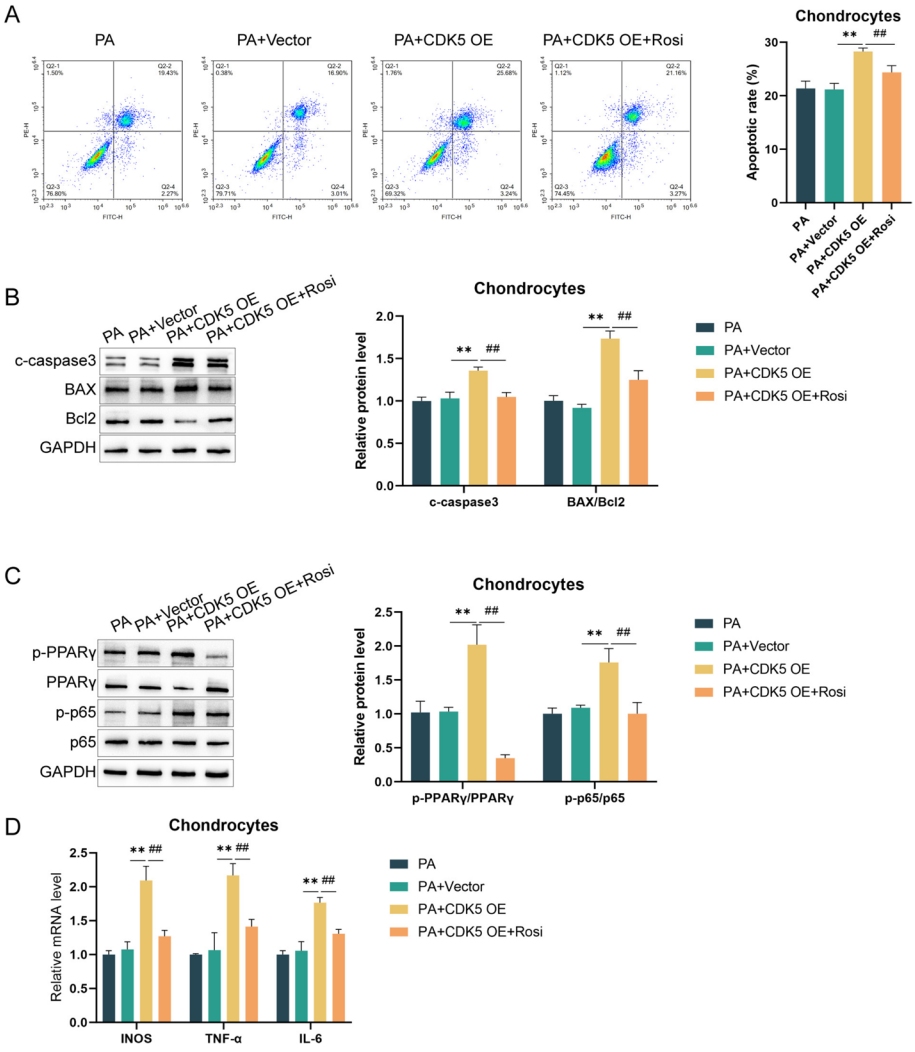

Fig. 8 PPARγ/NF-κB signaling mediates effects of CDK5 on PA-induced chondrocyte damage. Under PA treatment, mouse chondrocytes were transfected with CDK5 OE with or without treatment with Rosi (a PPARγ agonist inhibiting PPARγ phosphorylation at Ser273). **A** FC was performed to determine cell apoptosis. **B** Immunoblotting was performed to determine the protein levels of cleaved caspase-3, Bax, and Bcl2. **C** Immunoblotting was performed to determine PPARγ, p-PPARγ (Ser273), p-p65, and p65 protein levels in chondrocytes. **D** The levels of inflammatory factors INOS, TNF-α, and IL-6 within chondrocytes were detected by qRT-PCR. All $N = 3$ (biological replicates). $^{**}p < 0.01$; $\#\#p < 0.01$

overexpression-induced PPARγ phosphorylation at Ser273 and p65 phosphorylation in chondrocytes (Fig. 8C). Moreover, CDK5 overexpression notably promoted the levels of inflammatory factors INOS, TNF-α, and IL-6 within chondrocytes in comparison with the PA and PA + Vector group, whereas Rosi treatment decreased INOS, TNF-α, and IL-6 levels compared with the PA + CDK5 OE group (Fig. 8D).

CDK5 binds to PPARγ to regulate the NF-κB signaling pathway

Finally, whether CDK5 interacts directly with PPARγ to influence downstream NF-κB activation was investigated. Co-IP assays in both RAW264.7 macrophages and chondrocytes revealed a direct CDK5–PPARγ complex, which was significantly reduced following Rosi treatment (Supplementary Fig. S3A, B). Studies have shown that PPARγ promotes the expression of inhibitor of nuclear factor kappa-B alpha (IkBα), thereby

inhibiting p65 phosphorylation [31, 32]. In addition, PPARγ can bind to the promoter of IkBα as a transcription factor [33]. Hence, the effects of CDK5 on the IkBα level in macrophages and chondrocytes were explored. PCR results showed that, under PA treatment, a downregulation of IκBα mRNA occurred in both cell types upon CDK5 overexpression, with IκBα mRNA levels rescued by Rosi treatment (Supplementary Fig. S3C, D). Bioinformatic analysis using JASPAR identified high-affinity PPARγ binding motifs approximately 2 kb upstream of the IκBα promoter (Fig S3E). Functional ChIP-qPCR confirmed that CDK5 overexpression decreased PPARγ enrichment at the IκBα promoter, while Rosi treatment restored this binding in both macrophages and chondrocytes (Supplementary Fig. S3F, G). Correspondingly, luciferase reporter assays demonstrated that CDK5 overexpression suppressed IκBα transcriptional activity in both macrophages and chondrocytes, an effect that was reversed by Rosi treatment (Supplementary Fig. S3H, I). These findings demonstrate that CDK5 modulates NF-κB signaling by physically binding to PPARγ, disrupting PPARγ-mediated IκBα transcription, and promoting NF-κB activation.

Discussion

The main findings of the present study demonstrate that mechanical destabilization by DMM induces CDK5 expression in joint tissues, and that obesity further amplifies CDK5 activation, leading to exacerbated OA pathology. In vivo, CDK5 knockdown alleviates obesity-related OA by reducing inflammation and protecting cartilage integrity through PPARγ/NF-κB signaling. In vitro studies reveal that CDK5 modulates PA-induced polarization of macrophages and chondrocyte apoptosis. Mechanistically, CDK5 directly binds PPARγ and facilitates the phosphorylation of PPARγ at Ser273, then inhibiting PPARγ-dependent transcription of IκBα, which in turn unleashes the NF-κB pathway.

Obesity is the greatest modifiable OA risk factor [34–36]. Herein, analyses of synovial tissues of obese patients with OA exhibited pronounced hyperplasia and severe inflammatory infiltration, contrary to the mild synovial hyperplasia and moderate inflammatory cell infiltration found within nonobese patients with OA [37, 38]. Further assessment of cartilage tissues revealed severe cartilage matrix degradation within obese patients with OA, marked by extensive loss of proteoglycan content and significant structural damage, in contrast to the mild to moderate proteoglycan loss and early signs of degradation observed in nonobese patients with OA [39, 40]. These observations indicate that obesity significantly exacerbates synovial inflammatory infiltration and cartilage degradation in OA. Furthermore, HFD administration exacerbated DMM-induced synovial M1 macrophage infiltration and cartilage degradation in OA mice, supporting observations from human clinical samples. More importantly, elevated levels of CDK5 were observed in both synovial and cartilage tissues of obese patients with OA as well as in synovial and cartilage tissues of OA mice. CDK5 has been regarded as a mediator of PPARγ phosphorylation at Ser273, leading to decreased PPARγ activity [24, 25] and impaired PPARγ regulation of lipid metabolism and anti-inflammatory responses, thereby facilitating a pro-inflammatory state [24, 25]. These findings suggest that CDK5 might link obesity and OA progression by promoting inflammatory responses and cartilage degradation through modulation of the PPARγ pathway. It is worth noting that CDK5 expression was elevated in DMM-operated knees even in the absence of obesity, indicating that mechanical injury alone initiates CDK5 activation. However, mice

subjected to both HFD and DMM exhibited significantly higher CDK5 expression and more severe cartilage degeneration than the DMM-alone group, demonstrating that obesity acts as an amplifier, rather than the primary trigger. This pattern may suggest a two-step pathological model. DMM-induced cartilage damage may activate CDK5, while obesity-related inflammatory signaling may further boost CDK5/PPARγ activity, thereby exacerbating joint pathology.

To validate the hypothesis, an obese OA model was established in mice and CDK5 knockdown was conducted in model mice. In vivo studies demonstrated that CDK5 knockdown in obese OA mice led to significant reductions in cartilage damage, as well as synovial M1 macrophage infiltration. Reportedly, the apoptosis of chondrocytes could participate in articular cartilage damage within osteoarthritis and is associated with cartilage diseases; in OA, chondrocytes gain apoptotic and necrotic morphology [41]. M1 macrophages aggregated more within the synovial membrane of experimental OA compared with M2 macrophages and worsened OA development, whereas M2 macrophages might elicit cartilage synthesis and repress the apoptosis of chondrocytes [42–44]. Therefore, CDK5 might affect the severity of OA in obesity through synovial M1 macrophage infiltration and chondrocyte apoptosis. More importantly, the effects of CDK5 were associated with a decrease in the phosphorylation of PPARγ and NF-κB pathways, which are key players in inflammatory and apoptotic processes [45, 46]. Specifically, phosphorylation of PPARγ at Ser273 impairs its anti-inflammatory and lipid metabolic functions [24, 25]. Thus, CDK5 knockdown alleviated obesity-related OA by reducing inflammation and protecting cartilage integrity, possibly through PPARγ/NF-κB signaling.

In vitro studies with RAW264.7 macrophages and primary chondrocytes provided further support of our in vivo findings. In macrophages, CDK5 overexpression facilitated M1 polarization, marked by increased levels of inflammatory markers including INOS and TNF-α, while CDK5 knockdown promoted M2 polarization, characterized by anti-inflammatory markers including Arg-1 and IL-10 [47, 48]. This polarization shift was further supported by flow cytometer analysis, showing decreased $INOS^+/CD206^+$ ratios in CDK5-knockdown cells, indicating a shift toward an anti-inflammatory phenotype. In chondrocytes, CDK5 overexpression elevated apoptosis, as demonstrated by increased cleaved caspase-3 levels and Bax/Bcl-2 ratio, while its knockdown reduced apoptosis, suggesting that CDK5 knockdown decreases chondrocyte death in OA. These in vitro findings are similar to our earlier in vivo findings that CDK5 knockdown reduces cartilage damage and inflammation in obese OA mice by shifting macrophage polarization toward an anti-inflammatory phenotype (reducing synovial M1 macrophage infiltration) and protecting chondrocytes from apoptosis.

To further investigate the mechanism by which CDK5 exacerbates obesity-related OA, the study explored the effects of rosiglitazone, a PPARγ agonist that inhibits PPARγ phosphorylation at Ser273 [49], on CDK5-overexpressing macrophages and chondrocytes. Treatment with rosiglitazone in CDK5-overexpressing macrophages reduced the expression of M1 markers (INOS and TNF-α) and increased M2 markers (Arg-1 and IL-10), indicating a shift toward an anti-inflammatory phenotype. This was corroborated by a decreased $INOS^+/CD206^+$ macrophage ratio, demonstrating a balance toward M2 polarization. Similarly, in CDK5-overexpressing chondrocytes, rosiglitazone treatment reduced apoptosis and levels of proapoptotic markers, including cleaved caspase-3 and

Bax, while increasing the antiapoptotic marker Bcl-2 [50, 51]. These changes were associated with rosiglitazone-induced decreased phosphorylation of PPARγ at Ser273 and NF-κB p65 within both macrophages and chondrocytes, suggesting that rosiglitazone mitigates the pro-inflammatory and pro-apoptotic effects of CDK5 overexpression through inhibition of these phosphorylation events. Moreover, previous report have documented that CDK5 directly binds to PPARγ [52]. Our co-IP data similarly confirm this interaction in both cell types, supporting a conserved regulatory axis. PPARγ promotes the expression of IkBα, thereby inhibiting p65 phosphorylation [31, 32]. In addition, PPARγ can bind to the promoter of IκBα as a transcription factor [33]. Our ChIP assay confirmed that CDK5 overexpression decreased PPARγ enrichment at the IκBα promoter. Correspondingly, luciferase reporter assays demonstrated that CDK5 overexpression suppressed IκBα transcriptional activity. Hence, CDK5 binding to PPARγ impairs PPARγ's ability to induce IκBα transcription, thus relieving negative feedback on NF-κB p65 activity—a mechanism aligning with previous demonstrations that ligand-activated PPARγ promotes IκBα expression, thereby suppressing NF-κB-dependent inflammation [53]. In summary, our mechanism studies showed that CDK5 modulated NF-κB signaling by physically binding to PPARγ or facilitating PPARγ phosphorylation, disrupting PPARγ-mediated IκBα transcription, and promoting NF-κB activation.

This study has several limitations that should be considered. Firstly, the human cohort was small, comprising only six subjects per group with an unequal distribution of males and females, which may introduce sex-related biases. Additionally, our murine experiments utilized only male mice, potentially limiting the generalizability of our findings across sexes. Also, the use of high-fat diet-induced obesity in mice may not fully replicate the complex metabolic and inflammatory environment of human obesity. Future research should aim to include larger, sex-balanced cohorts and utilize both male and female animal models to assess sex-specific differences in the CDK5/PPARγ axis. Additionally, exploring alternative models of obesity, such as genetic or chemical-induced obesity, may provide a more comprehensive understanding of the disease mechanisms.

These findings confirm that CDK5 promotes inflammation and apoptosis in obesity-related OA by binding to PPARγ and facilitating the phosphorylation of PPARγ at Ser273 and activating the NF-κB pathway. Targeting this pathway with rosiglitazone could mitigate the effects of CDK5 overexpression in vitro and in vivo, providing a potential therapeutic strategy for managing OA in obese patients.

Conclusions

CDK5 promotes the progression of obesity-associated OA through the PPARγ/NF-κB pathway and is a potential therapeutic target in OA, especially in obese patients.

Abbreviations

ABC	Avidin–biotin complex
BCA	Bicinchoninic acid
BMI	Body mass index
CDK5	Cyclin-dependent kinase 5
ChIP	Chromatin immunoprecipitation
Co-IP	Co-immunoprecipitation
DAB	3,3′-Diaminobenzidine
DAPI	4′,6-Diamidino-2-phenylindole
DMEM/F12	Dulbecco's modified Eagle's medium/nutrient mixture F-12
DMM	Destabilization of the medial meniscus
ECL	Enhanced chemiluminescence
EDTA	Ethylenediaminetetraacetic acid

FBS	Fetal bovine serum
H&E	Hematoxylin and eosin
HFD	High-fat diet
IgG	Immunoglobulin G
IF	Immunofluorescence
IHC	Immunohistochemical
IL	Interleukin
NF-κB	Nuclear factor-κB
OA	Osteoarthritis
OARSI	Osteoarthritis Research Society International
OE	Overexpression
PA	Palmitic acid
PI	Propidium iodide
PPARγ	Peroxisome proliferator-activated receptor gamma
PS	Penicillin/streptomycin
PVDF	Polyvinylidene fluoride
qRT-PCR	Quantitative real-time reverse-transcriptase polymerase chain reaction
RIPA	Radioimmunoprecipitation assay
Rosi	Rosiglitazone
RT	Room temperature
SDS-PAGE	Sodium dodecyl sulfate-polyacrylamide gel electrophoresis
siRNA	Small interfering RNA
T-CHO	Total cholesterol
TG	Triglycerides
TNF-α	Tumor necrosis factor alpha

Supplementary Information

The online version contains supplementary material available at https://doi.org/10.1186/s11658-025-00822-7.

Additional file 1

Additional file 2

Additional file 3

Additional file 4

Additional file 5

Additional file 6

Additional file 7

Acknowledgements
Not applicable.

Author contributions
Yusheng Li: methodology, validation, formal analysis, investigation, data curation, writing-original draft preparation, writing—review and editing. Hengzhen Li: software, data curation, visualization, writing—review and editing. Xingfu Li: software, visualization, writing—review and editing. Xin Chen: software, visualization, writing—review and editing. Jingyue Su: software, visualization, writing—review and editing. Shengwu Yang: validation, writing—review and editing. Wenfeng Xiao: conceptualization, investigation, resources, supervision, project administration, funding acquisition, writing—review and editing. Zhenhan Deng: conceptualization, investigation, resources, supervision, project administration, funding acquisition, writing—review and editing. All authors approved the final version of the manuscript and agreed to be accountable for all aspects of the work.

Funding
The author(s) disclose receipt of the following financial or material support for the research, authorship, and/or publication of this article: Guangdong Basic and Applied Basic Research Foundation (2023A1515220072), the National Key R&D Program of China (no. 2023YFB4606705), the National Natural Science Foundation of China (nos. 82272611, 82072506, and 92268115), the Hunan Provincial Science Fund for Distinguished Young Scholars (no. 2024JJ2089), the Science and Technology Innovation Program of Hunan Province (no. 2023SK2024), the Natural Science Foundation of Hunan Province (no.2023JJ30949), the Program of Health Commission of Hunan Province (no. 202204074879), and the National Clinical Research Center for Geriatric Disorders (Xiangya Hospital, grant no. 2021KFJJ02).

Data availability
The data supporting this study's findings are available from the corresponding author upon reasonable request.

Declarations

Ethics approval and consent to participate
All clinical specimens used in this study were approved by the Medical Ethics Committee of the Shenzhen Second People's Hospital (no. 2024-102-01PJ, 21 March 2024). The Medical Ethics Committee of the Shenzhen Second People's

Hospital acts on the Helsinki Declaration. The animal experiment received approval from the Animal Ethics Committee of Peking University Graduate School (no. ER-0023-042, 17 January 2023). The Animal Ethics Committee of Peking University Graduate School acts on the International Council for Laboratory Animal Science (ICLAS).

Consent for publication
Not applicable.

Competing interests
The authors declare no competing interests.

Statement of role of funding source
Academic funding sources did not influence the project direction or decision to publish.

Clinical trial number
Not applicable.

Received: 19 February 2025 / Accepted: 15 October 2025
Published online: 13 November 2025

References

1. Murphy L, Schwartz TA, Helmick CG, Renner JB, Tudor G, Koch G, et al. Lifetime risk of symptomatic knee osteoarthritis. Arthritis Rheum. 2008;59(9):1207–13.
2. Orr C, Vieira-Sousa E, Boyle DL, Buch MH, Buckley CD, Canete JD, et al. Synovial tissue research: a state-of-the-art review. Nat Rev Rheumatol. 2017;13(8):463–75.
3. Liu Z, Xie W, Li H, Liu X, Lu Y, Lu B, et al. Novel perspectives on leptin in osteoarthritis: focus on aging. Genes Dis. 2024;11(6):101159.
4. Visser AW, de Mutsert R, le Cessie S, den Heijer M, Rosendaal FR, Kloppenburg M. The relative contribution of mechanical stress and systemic processes in different types of osteoarthritis: the NEO study. Ann Rheum Dis. 2015;74(10):1842–7.
5. van den Bosch MHJ, Blom AB, van der Kraan PM. Inflammation in osteoarthritis: our view on its presence and involvement in disease development over the years. Osteoarthritis Cartilage. 2024;32(4):355–64.
6. Su J, Sun X, Chen X, Wei K, Luo D, Yang S, et al. Cip2a promotes inflammation and exacerbates osteoarthritis by targeting CEMIP. Cell Mol Biol Lett. 2025;30(1):67.
7. Cai W, Yang T, Liu H, Han L, Zhang K, Hu X, et al. Peroxisome proliferator-activated receptor gamma (PPARgamma): A master gatekeeper in CNS injury and repair. Prog Neurobiol. 2018;163–164:27–58.
8. Huang G, Jiang W, Xie W, Lu W, Zhu W, Deng Z. Role of peroxisome proliferator-activated receptors in osteoarthritis (Review). Molecular medicine reports. 2021;23(2).
9. Harasymowicz NS, Clement ND, Azfer A, Burnett R, Salter DM, Simpson A. Regional differences between perisynovial and infrapatellar adipose tissue depots and their response to class II and class III obesity in patients with osteoarthritis. Arthritis Rheumatol. 2017;69(7):1396–406.
10. Fuentes E, Guzmán-Jofre L, Moore-Carrasco R, Palomo I. Role of PPARs in inflammatory processes associated with metabolic syndrome (review). Mol Med Rep. 2013;8(6):1611–6.
11. Vasheghani F, Monemdjou R, Fahmi H, Zhang Y, Perez G, Blati M, et al. Adult cartilage-specific peroxisome proliferator-activated receptor gamma knockout mice exhibit the spontaneous osteoarthritis phenotype. Am J Pathol. 2013;182(4):1099–106.
12. Vasheghani F, Zhang Y, Li YH, Blati M, Fahmi H, Lussier B, et al. PPARgamma deficiency results in severe, accelerated osteoarthritis associated with aberrant mTOR signalling in the articular cartilage. Ann Rheum Dis. 2015;74(3):569–78.
13. Fahmi H, Martel-Pelletier J, Pelletier JP, Kapoor M. Peroxisome proliferator-activated receptor gamma in osteoarthritis. Mod Rheumatol. 2011;21(1):1–9.
14. Xu H, Chen S, Meng C, He Y, Huang XJ, You HB. Inhibition of CC chemokine receptor 1 ameliorates osteoarthritis in mouse by activating PPAR-gamma. Mol Med. 2024;30(1):74.
15. Feng Z, Huang Q, Zhang X, Xu P, Li S, Ma D, et al. PPAR-gamma activation alleviates osteoarthritis through both the Nrf2/NLRP3 and PGC-1alpha/Deltapsi (m) pathways by inhibiting pyroptosis. PPAR Res. 2023;2023:2523536.
16. Ni S, Yi N, Yuan H, Li D, Chen X, Zhuang C. *Angelica sinensis* polysaccharide improves mitochondrial metabolism of osteoarthritis chondrocytes through PPARgamma/SOD2/ROS pathways. Phytother Res. 2023;37(11):5394–406.
17. Deng Z, Chen F, Liu Y, Wang J, Lu W, Jiang W, et al. Losartan protects against osteoarthritis by repressing the TGF-β1 signaling pathway via upregulation of PPARγ. J Orthop Translat. 2021;29:30–41.
18. Sharma AM, Staels B. Review: peroxisome proliferator-activated receptor gamma and adipose tissue–understanding obesity-related changes in regulation of lipid and glucose metabolism. J Clin Endocrinol Metab. 2007;92(2):386–95.
19. Roman-Blas JA, Jimenez SA. NF-kappaB as a potential therapeutic target in osteoarthritis and rheumatoid arthritis. Osteoarthritis Cartilage. 2006;14(9):839–48.
20. Bo QL, Chen YH, Yu Z, Fu L, Zhou Y, Zhang GB, et al. Rosiglitazone pretreatment protects against lipopolysaccharide-induced fetal demise through inhibiting placental inflammation. Mol Cell Endocrinol. 2016;423:51–9.
21. Song Y, Zhao H, Liu J, Fang C, Miao R. Effects of citral on lipopolysaccharide-induced inflammation in human umbilical vein endothelial cells. Inflammation. 2016;39(2):663–71.
22. Pfander P, Fidan M, Burret U, Lipinski L, Vettorazzi S. Cdk5 deletion enhances the anti-inflammatory potential of GC-mediated GR activation during inflammation. Front Immunol. 2019;10:1554.
23. Tiwari MN, Hall BE, Ton AT, Ghetti R, Terse A, Amin N, et al. Activation of cyclin-dependent kinase 5 broadens action potentials in human sensory neurons. Mol Pain. 2023;19:17448069231218352.
24. Li P, Fan W, Xu J, Lu M, Yamamoto H, Auwerx J, et al. Adipocyte NCoR knockout decreases PPARgamma phosphorylation and enhances PPARgamma activity and insulin sensitivity. Cell. 2011;147(4):815–26.

25. Teijeiro A, Garrido A, Ferre A, Perna C, Djouder N. Inhibition of the IL-17A axis in adipocytes suppresses diet-induced obesity and metabolic disorders in mice. Nat Metab. 2021;3(4):496–512.
26. Zhang X, Zhang R, Wang Y, Li L, Zhong Z. CDK5 Upregulated by ELF3 Transcription Promotes IL-1beta-induced Inflammation and Extracellular Matrix Degradation in Human Chondrocytes. Cell Biochem Biophys. 2024.
27. Deng Z, Gao X, Sun X, Amra S, Lu A, Cui Y, et al. Characterization of articular cartilage homeostasis and the mechanism of superior cartilage regeneration of MRL/MpJ mice. FASEB J. 2019;33(8):8809–21.
28. Li X, Zhang Z, Xie J, Guo W, Deng Z, Huang Z. Deficiency of cartilage-specific Y-box binding protein 1 represses NF-κB signaling and alleviates osteoarthritis progression. Arthritis Rheumatol. 2025.
29. Li X, Lu W, Ni L, Su J, Wang D, Deng Z. Mitochondria-rich extracellular vesicles derived from the culture supernatant of human synovial fluid-derived mesenchymal stem cells inhibited senescence of stressed/inflammatory licensed chondrocytes and delayed osteoarthritis progression. Int Immunopharmacol. 2025;147:113954.
30. Krenn V, Morawietz L, Burmester GR, Kinne RW, Mueller-Ladner U, Muller B, et al. Synovitis score: discrimination between chronic low-grade and high-grade synovitis. Histopathology. 2006;49(4):358–64.
31. Korbecki J, Bobiński R, Dutka M. Self-regulation of the inflammatory response by peroxisome proliferator-activated receptors. Inflamm Res. 2019;68(6):443–58.
32. Gong MX, Wei JJ, Yi Y, Liu X, Hou FQ, Li YQ, et al. Targeting PPARα/γ by icariside II to rescue GalN/LPS-induced acute liver injury in mice: involvement of SIRT6/NF-κB signaling pathway. Phytomedicine. 2025;136:156250.
33. Wu H, Wu L, Luo L, Wu YT, Zhang QX, Li HY, et al. Quercetin inhibits mitophagy-mediated apoptosis and inflammatory response by targeting the PPARγ/PGC-1α/NF-κB axis to improve acute liver failure. Int Immunopharmacol. 2024;143(Pt 2):113444.
34. Nedunchezhiyan U, Varughese I, Sun AR, Wu X, Crawford R, Prasadam I. Obesity, inflammation, and immune system in osteoarthritis. Front Immunol. 2022;13:907750.
35. King LK, March L, Anandacoomarasamy A. Obesity & osteoarthritis. Indian J Med Res. 2013;138(2):185–93.
36. Raud B, Gay C, Guiguet-Auclair C, Bonnin A, Gerbaud L, Pereira B, et al. Level of obesity is directly associated with the clinical and functional consequences of knee osteoarthritis. Sci Rep. 2020;10(1):3601.
37. Pearson MJ, Herndler-Brandstetter D, Tariq MA, Nicholson TA, Philp AM, Smith HL, et al. *IL*-6 secretion in osteoarthritis patients is mediated by chondrocyte-synovial fibroblast cross-talk and is enhanced by obesity. Sci Rep. 2017;7(1):3451.
38. Yao Z, Qi W, Zhang H, Zhang Z, Liu L, Shao Y, et al. Down-regulated GAS6 impairs synovial macrophage efferocytosis and promotes obesity-associated osteoarthritis. Elife. 2023. https://doi.org/10.7554/eLife.83069.
39. Chen L, Yao F, Wang T, Li G, Chen P, Bulsara M, et al. Horizontal fissuring at the osteochondral interface: a novel and unique pathological feature in patients with obesity-related osteoarthritis. Ann Rheum Dis. 2020;79(6):811–8.
40. Sun AR, Udduttula A, Li J, Liu Y, Ren PG, Zhang P. Cartilage tissue engineering for obesity-induced osteoarthritis: physiology, challenges, and future prospects. J Orthop Translat. 2021;26:3–15.
41. Salucci S, Falcieri E, Battistelli M. Chondrocyte death involvement in osteoarthritis. Cell Tissue Res. 2022;389(2):159–70.
42. Zhang H, Lin C, Zeng C, Wang Z, Wang H, Lu J, et al. Synovial macrophage M1 polarisation exacerbates experimental osteoarthritis partially through R-spondin-2. Ann Rheum Dis. 2018;77(10):1524–34.
43. Dai M, Sui B, Xue Y, Liu X, Sun J. Cartilage repair in degenerative osteoarthritis mediated by squid type II collagen via immunomodulating activation of M2 macrophages, inhibiting apoptosis and hypertrophy of chondrocytes. Biomaterials. 2018;180:91–103.
44. Ma Y, Yang H, Zong X, Wu J, Ji X, Liu W, et al. Artificial M2 macrophages for disease-modifying osteoarthritis therapeutics. Biomaterials. 2021;274:120865.
45. Croasdell A, Duffney PF, Kim N, Lacy SH, Sime PJ, Phipps RP. Ppargamma and the innate immune system mediate the resolution of inflammation. PPAR Res. 2015;2015:549691.
46. Liu T, Zhang L, Joo D, Sun SC. NF-kappaB signaling in inflammation. Signal Transduct Target Ther. 2017;2:17023.
47. Shapouri-Moghaddam A, Mohammadian S, Vazini H, Taghadosi M, Esmaeili SA, Mardani F, et al. Macrophage plasticity, polarization, and function in health and disease. J Cell Physiol. 2018;233(9):6425–40.
48. He C, Carter AB. The metabolic prospective and redox regulation of macrophage polarization. J Clin Cell Immunol. 2015. https://doi.org/10.4172/2155-9899.1000371.
49. Choi JH, Banks AS, Estall JL, Kajimura S, Bostrom P, Laznik D, et al. Anti-diabetic drugs inhibit obesity-linked phosphorylation of PPARgamma by Cdk5. Nature. 2010;466(7305):451–6.
50. Lomonosova E, Chinnadurai G. BH3-only proteins in apoptosis and beyond: an overview. Oncogene. 2008;27 Suppl 1(Suppl 1):S2–19.
51. Siddiqui WA, Ahad A, Ahsan H. The mystery of BCL2 family: Bcl-2 proteins and apoptosis: an update. Arch Toxicol. 2015;89(3):289–317.
52. Quan Q, Qian Y, Li X, Li M. Pioglitazone reduces β amyloid levels via inhibition of PPARγ phosphorylation in a neuronal model of Alzheimer's disease. Front Aging Neurosci. 2019;11:178.
53. Scirpo R, Fiorotto R, Villani A, Amenduni M, Spirli C, Strazzabosco M. Stimulation of nuclear receptor peroxisome proliferator-activated receptor-γ limits NF-κB-dependent inflammation in mouse cystic fibrosis biliary epithelium. Hepatology. 2015;62(5):1551–62.

Publisher's Note